Pergamon

PII: S1352-2310(96)00122-7

Atmospheric Environment Vol. 30, No. 23, pp. 3987–3993, 1996

1352-2310/96 $15.00 + 0.00

ON THE NATURE OF AIR POLLUTION DYNAMICS IN MEXICO CITY—I. NONLINEAR ANALYSIS

G. B. RAGA and L. LE MOYNE

Centro de Ciencias de la Atmósfera, UNAM, Ciudad Universitaria, 04510 México, DF, México

(*First received* 19 *December* 1995 *and in final form* 22 *March* 1996)

Abstract—We have applied a nonlinear dynamic analysis to air quality data (ozone, carbon monoxide, nitrous oxide and sulfur dioxide) obtained at 13 of the surface stations of the automated monitoring network in Mexico City, following the work of Li *et al.* (1994, *Atmospheric Environment* **28**, 1707–1714). The time series used consisted of hourly data obtained during 1993. The analysis has helped to identify the nature of the dynamics of ozone production and we have determined the number of degrees of freedom of the system. Interestingly, this value varied with location within the city, ranging from two (at a station located downtown) to eight. We suggest that this difference may be linked to variations in local orography that forces a vortex-type circulation within the basin throughout the year. Copyright © 1996 Elsevier Science Ltd

Key word index: Air quality, Mexico City, chaos theory analysis.

1. INTRODUCTION

The problem of air pollution in Mexico City has become a serious health threat for its inhabitants. The problem has very particular characteristics because the city is located 2.2 km above sea level and at approximately 19°N. It therefore, receives more solar radiation than other large cities located at sea level and in sub-tropical and mid-latitude regions. This incident solar radiation is very important in the ozone formation process in the boundary layer. The extremely high emissions (both by mobile and industrial sources) aggravate the problem dramatically throughout the year.

During the winter months, which occur during the dry season (October–May), the boundary layer becomes very stable during the night due to radiational cooling from the surface in cloudless sky conditions. Pollutants (emitted preferably during the daytime) can become trapped close to the surface in the early morning hours. As the day progresses, the stable boundary layer becomes unstable due to heating from solar radiation and grows, and pollutant concentrations become diluted. Nevertheless, it is often observed that events of extreme thermal stability (usually associated with very light or no wind) are directly linked to very high ozone concentrations. Because high emissions are initiated when the boundary layer is stably stratified, there is ample time for photochemical conversions from ozone precursors to occur.

During summer months, solar heating at the surface drives a convective boundary layer, with large clouds developing most days. Ventilation of the boundary layer is, thus, quite efficient by these convective plumes. Often these clouds precipitate and pollutants are substantially scavenged by the falling precipitation particles. Also gases are incorporated into cloud droplets within the clouds. Therefore, convection and precipitation contribute to the effective removal of gases and particles during the wet season (June–September). Nevertheless, when large scale conditions are appropriate (such as a high-pressure region affecting the Mexico City basin), extremely high values of surface ozone are also recorded during spring and summer.

The primary pollution problem in Mexico City has been identified as the formation of photochemical smog, in particular ozone. This oxidant is formed in the atmosphere by chemical reactions involving nitrogen oxides and volatile organic compounds in the presence of solar radiation. The particular conditions of gaseous emissions in Mexico City are such that the reactivity of precursor gases is enhanced. A reduction of visibility is also associated with the formation of photochemical aerosol particles. Because of their oxidizing properties, photochemical oxidants accelerate the conversion of sulfur dioxide into sulfates, which in turn interact with radiation decreasing the intensity reaching the surface.

In the present study we approach the problem of air pollution in Mexico City from the point of view of dealing with a highly nonlinear system in both the chemistry and the dynamics. We try to gain some understanding on the problem by performing a nonlinear dynamics analysis utilizing time series of ozone,

carbon monoxide and sulfur dioxide, obtained from surface monitoring stations.

Given the large number of inhabitants and the serious health effects that pollution has on their lives, it is extremely important to understand the dynamics of ozone formation, and this would lead to problem mitigation and eventually its prediction.

2. DESCRIPTION OF THE ANALYSIS METHOD

We have followed the methodology described by Li *et al.* (1994), which has become fairly standard in nonlinear time series analysis. We briefly describe it here, for completeness. The key to the analysis is the assumption that even if the exact description of the dynamical system under study is unknown, its phase space can be reconstructed by a single variable time series, as detailed in Packard *et al.* (1980). If an attractor, which describes the asymptotic behavior of the dynamical system, for the problem exists in phase space, then the dimension of the attractor will provide a measure of the minimum number of independent variables that fully describe the dynamical system. If $x_0(t)$ is the time series of one of the variables in a system represented by n first-order differential equations, then the system can be transformed to an nth order differential equation for the single variable $x_0(t)$ and the derivatives of the original time series can be estimated based on a de-correlation time lag. The parameter n corresponds to the embedded dimension.

The goal is to determine the correlation dimension of the attractor (if it exists) from the original time series, and thus, the number of degrees of freedom. The procedure utilized has been described by Grassberger and Procaccia (1983). A correlation coefficient can be constructed in phase space as:

$$C(r) = \lim_{N\to\infty} \frac{1}{(N^2 - N)} \sum_{\substack{i,j=1 \\ i\neq j}}^{N} H(r - |\mathbf{x}_i - \mathbf{x}_j|) \quad (1)$$

where H is the Heaviside function and r is an arbitrary distance in phase space. For sufficiently small value of r (Grassberger and Procaccia, 1983), the correlation coefficient will follow a power law:

$$C(r) \sim r^D \quad (2)$$

The correlation dimension D can be easily determined and it provides an unambiguous distinction between random and deterministic behavior, when it is plotted as a function of the embedded dimension n.

The method described above has been increasingly applied to the analysis of a variety of time series to study the dynamic behavior of the atmosphere. A wide range of values (from 2 to 9) for the correlation dimension have been obtained (Nicolis and Nicolis, 1984; Osborne *et al.*, 1986; Tsonis and Elsner, 1988; Keppenne and Nicolis, 1989), results that indicate no saturation of this dimension (Grassberger, 1986; Fraedrich, 1986). Islam *et al.* (1993) point out that caution should be exercised when interpreting the correlation dimensions obtained through this method. They argue that unrealistically low values have been obtained for the atmosphere (based on analysis of precipitation or sunshine duration) because such time series may be constrained by the presence of thresholds.

3. OBSERVATIONS

Mexico City has an automated network for atmospheric monitoring (Red Automatica de Monitoreo Ambiental, RAMA, operated by Departamento del Distrito Federal) that consists of 25 surface-based stations in which thermodynamic, dynamic and chemical parameters are measured hourly. Not all stations measure all the parameters mentioned, and some of them also measure particles (total and smaller than 10 μm). The chemical species measured are ozone (O_3), carbon monoxide (CO), sulfur dioxide (SO_2) and nitrogen oxides (NO_x). Figure 1 presents a map of the Mexico City basin showing all the surface stations denoted by letters. The stations that have been selected for this study correspond to letters C, F, G, L, N, P, Q, T, U, W, X, Y and Z. Also shown are topography contours (400 m intervals) and the extent of the urban area. Most of the stations are in an urban setting, except for M and N which are located close to Lake Texcoco and just outside of the main populated areas.

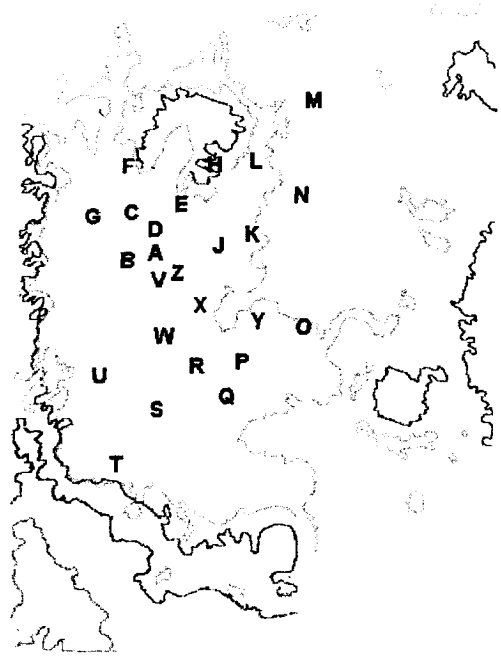

Fig. 1. Map of Mexico City showing all RAMA stations, topography contours (every 400 m) and extent of urban area.

The instrumentation in the RAMA stations follows the guidelines set forth by the U.S. Environmental Protection Agency (EPA, 1983) and are frequently calibrated. The measuring principle for ozone is based on the chemiluminescent reaction of ozone with ethylene. The resulting photocurrent is amplified and then recorded. Carbon monoxide is measured by nondispersive infrared photometry, quantifying the absorption of CO by a suitable detector. Sulfur dioxide is measured utilizing the pararosaniline method. A chemical reaction is induced in which the optical density at a particular concentration is determined and related directly to the amount of SO_2 present in the air sample. And finally, nitrogen oxides (NO_x) are determined by gas-phase chemiluminescence and the concentration of NO_2 is determined by subtraction. Data quality is generally good and the time series for 1993 are fairly complete, especially for CO and O_3 (about 80% on average).

4. RESULTS AND DISCUSSION

4.1. *Linear analysis*

Table 1 shows the annual geometric mean and standard deviation for O_3, SO_2, CO and NO_2 in the selected stations. The NO_2 time series have a significant fraction of the data missing (at least 70% of datapoints were required) and have not therefore been used in any further statistical analysis. Note the low O_3 values observed in station W, located downtown.

Figure 2 shows a segment of the time series observed at station T during March for O_3, NO_2 and SO_2. The O_3 time series clearly shows a repeatable diurnal cycle, with peak concentrations occurring during the early to mid-afternoon. Concentrations reached levels of 0.3 ppm during this period, exceeding substantially the air quality standard for ozone (0.11 ppm for more than 1 h). The pattern of an observed peak in the mid-afternoon hours is repeated daily in all monitoring stations, throughout the year. It is also clear from the figure that NO_2 concentrations drop sharply when O_3 builds up (coinciding with a decrease in NO levels after rush hour), and then recover in the late afternoon. The O_3 concentration is not related directly to the SO_2 concentrations, which do not present the regularity of the O_3 and NO_2 time series.

The O_3 time series were Fourier transformed to determine the frequencies contributing most of the energy. Figure 3 presents a typical example where it is possible to identify the diurnal oscillations with large harmonics at 12 and 8 h.

Cross-correlations between stations were computed for SO_2 and CO time series. The results for both variables indicate that there is a marked pattern of higher correlation coefficients in the western part of the city (Fig. 4). The cross-correlations calculated with a time lag of 1 to 4 h indicate that there is a tendency for the higher correlations to move from the northwest to the southeast, along the western border of the city. This pattern was first pointed out by Jauregui *et al.* (1981), utilizing SO_2 concentrations measured in January 1976, within the dry season. The pattern is more clearly seen in SO_2 during the dry season, due to the fact that SO_2 is rapidly depleted when the relative humidity is high and in the presence of clouds. The results obtained using CO (which is a more conserved tracer) are in general agreement with the SO_2 ones, suggesting that there is a predominant pattern of transport within the city throughout the year.

4.2. *Nonlinear analysis*

The autocorrelation analysis for all 13 stations indicated that a time lag of 5 h would give uncorrelated time series. In contrast, Li *et al.* (1994), utilize a decorrelation lag of 1 h, which at least in the conditions

Table 1. Geometric mean, standard deviation and percentage of datapoints present for ozone, nitrogen dioxide, sulfur dioxide and carbon monoxide during 1993 in all stations considered

	O_3 ($\times 10^{-2}$ ppm)			NO_2 ($\times 10^{-1}$ ppm)			SO_2 ($\times 10^{-2}$ ppm)			CO (ppm)		
Station	μ	σ	%	μ	σ	%	μ	σ	%	μ	σ	%
C	4.45	5.27	70				2.38	2.35	67			
W	1.56	3.23	84	0.28	0.25	64				2.76	2.20	91
Q	3.13	4.39	76	0.38	0.22	81	1.39	1.48	49	3.06	2.26	74
G	3.82	4.82	72	0.25	0.32	46	1.32	1.77	73	2.49	2.50	86
D										2.05	2.31	71
Y	2.75	4.60	85	0.37	0.25	58	2.48	2.26	61			
Z	3.19	4.88	81							2.97	2.61	83
X	2.65	5.23	84	0.51	0.28	79	1.74	2.16	81	3.05	2.59	85
T	3.12	5.76	91	0.37	0.25	85	0.09	1.44	75	2.13	1.68	87
U	2.67	5.70	84							3.10	2.50	85
N	3.71	2.97	70	0.30	0.16	56	1.18	1.41	59			
F	4.01	4.11	83	0.28	0.27	63	1.65	1.99	78	2.65	2.27	85
P	3.09	4.85	81							2.16	2.40	75
L	3.79	3.76	77	0.40	0.26	68	1.84	2.74	69	2.82	2.73	78

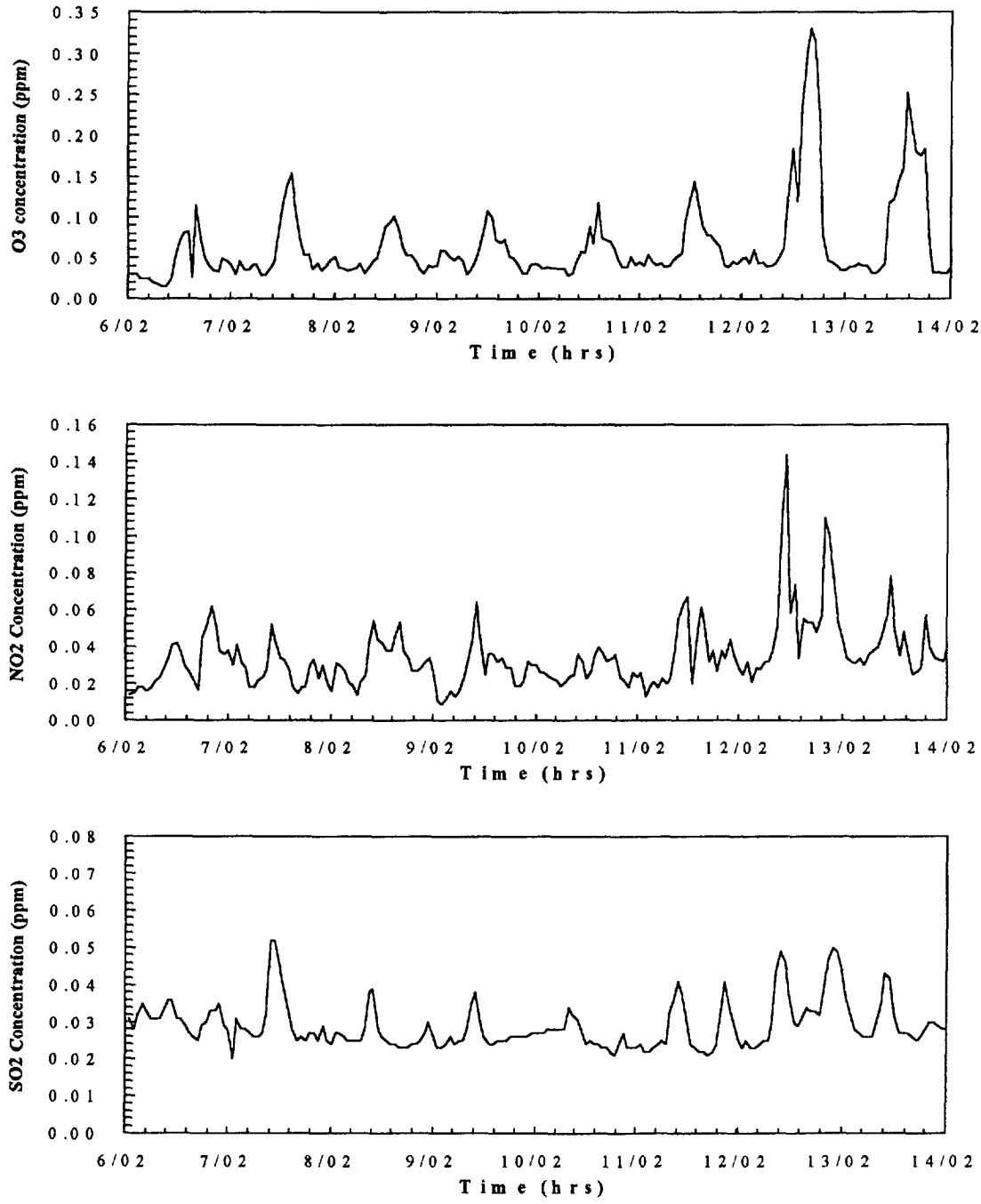

Fig. 2. Time series of O_3 (a), NO_2 (b) and SO_2 (c) for the period 9–14 March 1993 in station T.

observed in Mexico City does not guarantee time decorrelation. The correlation coefficient (from equation (3)) is computed for a range of embedded dimension from 2 to 20. Figure 5 shows the correlation coefficient as a function of the arbitrary distance r, for $n = 2, ..., 10$, obtained for station T. The slope of these curves, for small values of r, gives an estimate of the correlation dimension. A linear fit was applied to the segment with r between 0.001 and 0.05. The values obtained for the slope as a function of the embedded dimension are presented in Fig. 6, where it is clear that the O_3 dynamics is not a random process. The sensitivity to the choice of embedded dimension (10: triangles, or 20: diamonds) is shown, suggesting that $n = 10$ was almost enough to determine the correlation dimension. Nevertheless, the correlation dimension in all stations was calculated using $n = 20$. Figure 7 shows the degrees of freedom determined for

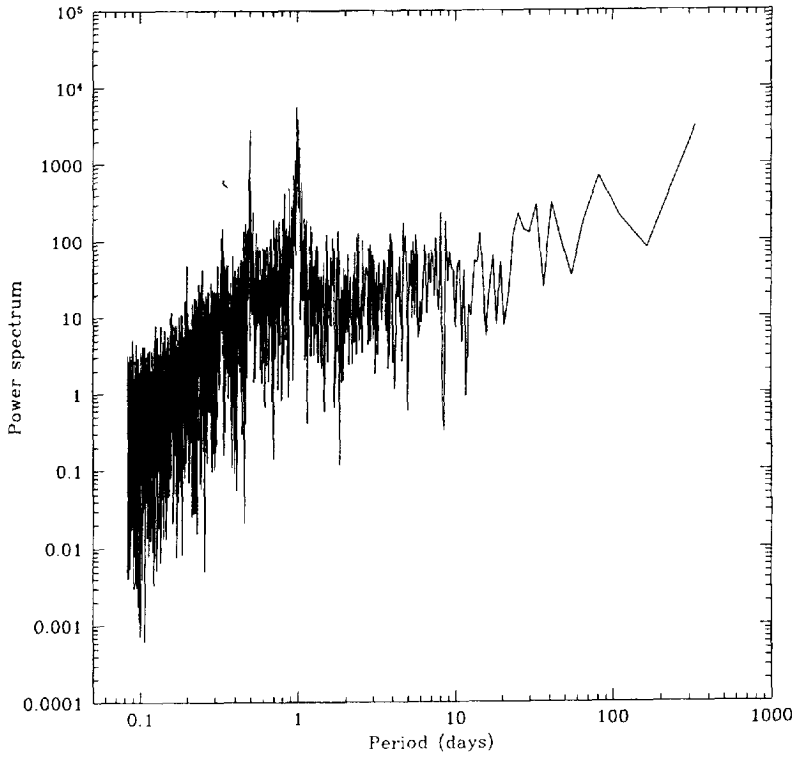

Fig. 3. Power spectrum of O_3 time series in station T.

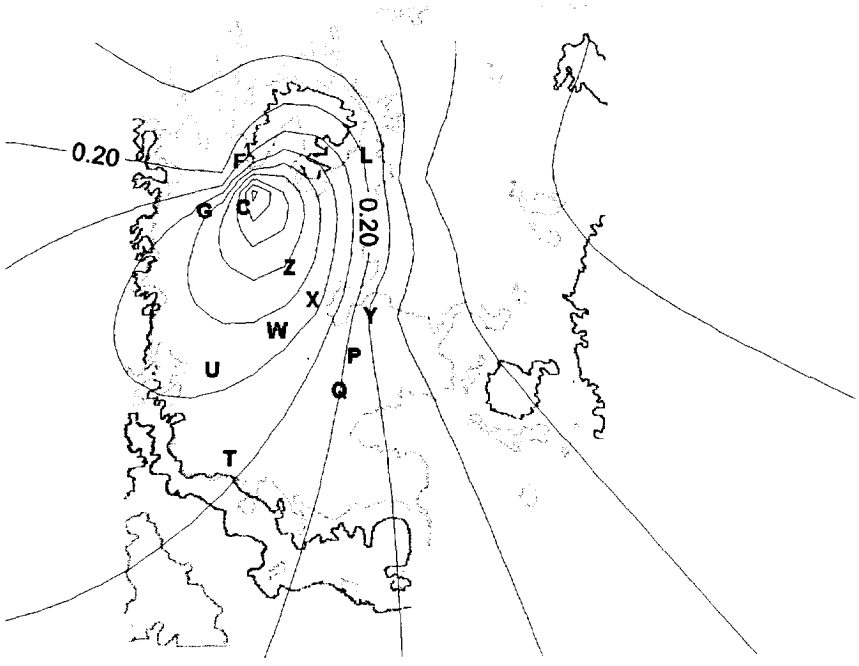

Fig. 4. Cross-correlation coefficient map for SO_2 with lag 0.

all the stations considered. There is a clear minimum in the center and towards the west. The lowest value determined was two, at station W. It is important to note that the observed O_3 values in this station are consistently lower than in all other stations (see Table 1). Inspection of the site indicates that a large building is located about 15 m to the N of the station. It is possible that the proximity of this building generates

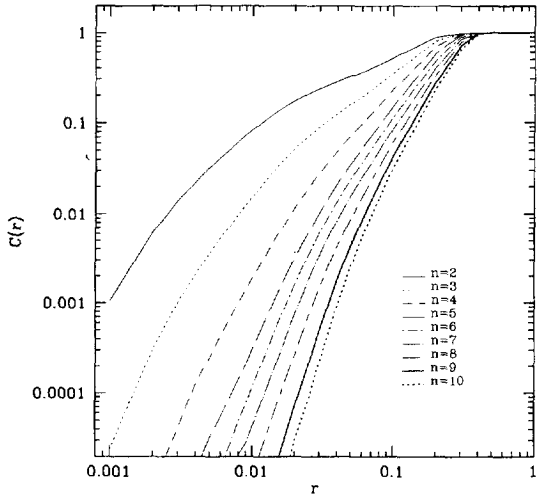

Fig. 5. Correlation coefficient (from equation (3)) as a function of the arbitrary distance in phase space r, for embedded dimension n ranging from 2 to 10, calculated using O_3 data from station T.

small scale eddies that are responsible for consistently underestimating O_3 concentrations. It may also be possible that this station is at the center of a wind vortex determined by the local topography, which would be consistent with the results from the cross-correlation analysis. In a companion paper (Le Moyne and Raga, 1996), we study a few high concentration events in detail and address the possibility of a vortical circulation within the urban basin.

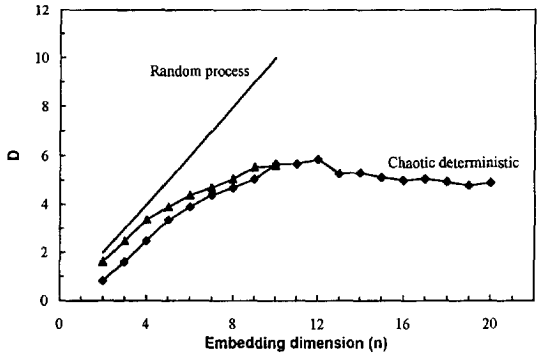

Fig. 6. Correlation dimension D as a function of the embedded dimension n, calculated using O_3 data from station L.

The O_3 time series were Fourier analyzed as was mentioned above, and among the several key frequencies identified, the contribution to the diurnal oscillation was removed. The time series was then inverse transformed back into physical space without the diurnal cycle. The nonlinear analysis was repeated utilizing the reconstructed O_3 time series. The number of degrees of freedom decreased by one in all the stations considered, consistent with removing one of the physical factors (e.g. solar radiation) that directly contribute to O_3 formation.

The O_3 time series for 1993 were partitioned into two subsets, corresponding to a dry season (March, April and May) and a rainy season (August, September and October). The nonlinear analysis was

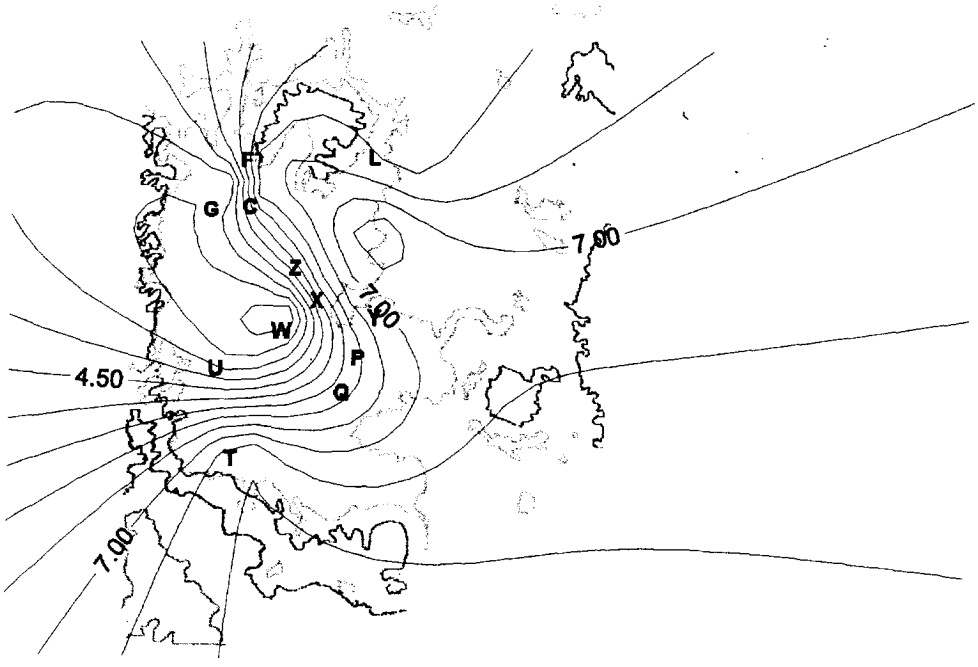

Fig. 7. Contour map of degrees of freedom obtained utilizing the 13 stations indicated.

repeated and one degree of freedom less was obtained from the dry subset, consistent with removing the contribution of the annual cycle to the system. The rainy season time series exhibits larger variability than the dry season one, due to the added variability introduced by precipitation. It is still possible to determine the degrees of freedom from the rainy season subset (one degree less than the full time series), but the correlation dimension does not reach saturation as smoothly as when using the full time series.

5. CONCLUSIONS

We have analyzed data from 13 stations of the surface monitoring network in Mexico City for 1993. A linear analysis of spatial cross-correlations has indicated a preferred pattern of transport within the city from the NW to the SE, along the western edge of the city and clearly not through the center of it. The nonlinear analysis performed indicates that there are fewer degrees of freedom in the center and western parts of the city, suggesting that perhaps the circulations are limited or forced. We propose that a vortex-type circulation may be present throughout the year within the city, given the particular topography that surrounds it. In a companion paper we explore more fully this hypothesis.

Acknowledgements—We are grateful to R. M. Ayala and C. Contreras for help with the figures and to T. Morales for helpful discussions. We are indebted to Dr I. Rosas for providing us with the data utilized for the analysis. This research was partially supported by the program Fondo de Apoyo a la Investigacion Basica y Tecnologica en Forma Mancomunada con las Instituciones de Educacion Superior (FIES).

REFERENCES

EPA (1983) Course 435 atmospheric sampling. United States Environmental Protection Agency, Report EPA 450/2-80-004.

Fraedrich K. (1986) Estimating the dimensions of weather and climate attractors. *J. atmos. Sci.* **43,** 331–344.

Grassberger P. (1986) Do climatic attractors exist? *Nature* **323,** 609–642.

Grassberger P. and Procaccia I. (1983) Measuring the strangeness of strange attractors. *Physica* **9D,** 189–208.

Islam S., Bras R. and Rodriguez-Iturbe I. (1993) A possible explanation for low correlation dimension estimates for the atmosphere. *J. appl. Met.* **32,** 203–208.

Jauregui E., Klaus D. and Lauer W. (1981) Una primera estimacion del transporte de SO_2 sohe la cindad de Mexico. *Geofis. Int.* **20,** 55–79

Keppenne C. and Nicolis C. (1989) Global properties and local structures of the weather attractors over Western Europe. *J. atmos. Sci.* **46,** 2356–2370.

Le Moyne L. and Raga G. B. (1996) On the nature of air pollution dynamics in Mexico City. Part II: case studies. To be submitted to *Atmospheric Environment.*

Li I.-F., Biswas P. and Islam S. (1994) Estimation of the dominant degrees of freedom for air pollutant concentration data: applications to ozone measurements. *Atmospheric Environment* **28,** 1707–1714.

Nicolis C. and Nicolis G. (1984) Is there a climatic attractor? *Nature* **353,** 241–244.

Osborne A., Kirwan A., Provenzale A. and Bergamasco L. (1986) A search for chaotic behaviour in large and mesoscale motions in the Pacific Ocean. *Physica* **23D,** 75–83.

Packard N. H., Crutchfield J. P., Farmer J. D. and Shaw R. S. (1980) Geometry from a time series. *Phys. Rev. Lett.* **45,** 712–716.

Tsonis A. and Elsner J. (1988) The weather attractor over very short timescales. *Nature* **333,** 545–547.